Visual identification of gut bacteria and determination of natural inhibitors using a fluorescent probe selective for PGP-1

Chao Wang[1,a,b], Zhenhao Tian[1,c], Ming Zhang[b,d], Ying Deng[b], Xiangge Tian[a], Lei Feng***[a,e], Jingnan Cui[d], Tony D. James**[e,f], Xiaochi Ma*[a]

[a] Institute of precision medicine and transformation, Second Affiliated Hospital, Dalian Medical University, Dalian 116023, China

[b] Dalian Key Laboratory of Metabolic Target Characterization and Traditional Chinese Medicine Intervention, College of Integrative Medicine, College of Pharmacy, Dalian 116044, China

[c] School of Life Sciences, Northwestern Polytechnical University, Xi'an 710072, China

[d] State Key Laboratory of Fine Chemicals, Dalian University of Technology, Dalian 116024, China

[e] School of Chemistry and Chemical Engineering, Henan Normal University, Xinxiang 453007, China

[f] Department of Chemistry, University of Bath, Bath BA2 7AY, UK

[1] These authors contributed equally to this work.

*Corresponding authors

**Corresponding authors

***Corresponding authors

E-mail: leifeng@dmu.edu.cn (L. Feng), t.d.james@bath.ac.uk (T.D. James), maxc1978@163.com (X. Ma)

ABSTRACT

PGP-1 is a bacterial hydrolase that can hydrolyze the amide bond of the L-pyroglutamate (L-pGlu) residue at the amino terminus of proteins and peptides. Guided by the biological function of PGP-1, an off-on NIR fluorescent probe **DDPA** was developed for the visual sensing of PGP-1 by conjugating pyroglutamic acid (recognition group) and **DDAN** (fluorophore). Using intestinal bacteria cultivation, eight bacteria strains with active PGP-1 were identified and cultivated efficiently using **DDPA**. In addition, three natural inhibitors against PGP-1 were isolated from the medical herb *Psoralea corylifolia*, which could be used to interfere with bacterial metabolism in the gut. As such, the fluorescent probe **DDPA** provides an efficient method and potential tool for the investigation of intestinal microbiota.

Keywords: PGP-1; Fluorescent probe; **DDPA**; Intestinal bacteria; High throughput screening

1. Introduction

Intestinal microbiota refers to the plethora of microorganisms that inhabit the human gastrointestinal tract.[1-3] Increasingly links between intestinal microbiota and human health and diseases have been uncovered.[4-6] Research has indicated that metabolites from gut microbiota play key roles in the biological processes of the host.[7, 8] As such, the metabolism of endogenous and exogenous substances by biological enzymes from gut microorganisms has attracted significant attention.[9-11]

Among various biological enzymes, pyroglutamyl aminopeptidase I (PGP-1, EC 3.4.19.3) is an important peptide metabolic enzyme that is expressed in bacteria, such as *Helcococcus ovis*, *Enterococci* and *Streptococcus pyogenes*, *Bacillus amyloliquefaciens*, and Enterobacteriaceae.[12-15] PGP-1 is a cytosolic cysteine peptidase, that specifically removes the L-pyroglutamate (L-pGlu) residue from the amino terminus of L-pGlu proteins and peptides.[16, 17] PGP-1 mediates the metabolism of thyrotropin-releasing hormone (TRH) and luteinizing hormone releasing hormone (LH-RH) *in vivo*, along with controlling hormonal signals.[18, 19] In the gastrointestinal tract, gastrin and neurotensin are peptides that also possess the L-pGlu residue, which can be hydrolyzed by PGP-1 derived from intestinal bacteria. Consequently, gastrointestinal bacteria with PGP-1 expression participate in the metabolism of endogenous biological peptides, which can interfere with the physiological status of humans. In consideration of the important functions of the intestinal bacteria with active PGP-1, the identification and cultivation of target bacteria are important for investigating the interaction between bacteria and the host. While, the inhibitors of PGP-1 from bacteria are anticipated to interfere with the metabolism of peptides mediated by intestinal bacteria.

Until now, the activity of mammalian PGP-1 has been determined using a colorimetric assay and several fluorescent probes.[20-23] However, only a few fluorescent probes with suitable fluorescence properties have been developed for

the visual detection of bacterial PGP-1, and the identification of inhibitors for PGP-1.

Fluorescent probes with high sensitivity have been developed for the real time sensing of biological enzymes from various species, including mammals, fish, fungi, and bacteria.[24-35] Hence, we decided to use 7-amino-1,3-dichloro-9,9-dimethylacridin-2(9*H*)-one (**DDAN**) as a near-infrared (NIR) fluorophore, to develop the fluorescent probe **DDPA** for the visual sensing of bacterial PGP-1 using pyroglutamic acid as the targeting group for PGP-1. Using **DDPA** as an activity assay for PGP-1, a high throughput screening method for natural inhibitors was established successfully. Furthermore, **DDPA** was used for the identification of intestinal bacteria with PGP-1 expression from human feces.

2. Experimental

2.1. Materials and apparatus

The nutrient broth medium for bacterial cultivation was purchased from Qingdao Haibo Biotechnology Co. Ltd. (China). The agar, glucose, Na_2HPO_4, NaH_2PO_4 were produced by Dalian Meilun Biotechnology Co., Ltd (China). The chemical reagents for the synthesis of the fluorescent probe such as hexane, ethyl acetate, dichloromethane, acetonitrile, and methanol were purchased from Tianjin Kemio Chemical Reagent Co., Ltd. Recombinant human carboxylesterases (CE1b, CE1c, and CE2) and CYP4F2 were purchased from Corning Incorporated Life Sciences. Lipase, leucine aminopeptidase (LAP), aminopeptidase N (APN), penicillin G acylase (PGA), γ-glutamyl-transferase (GGT), bovine serum albumin (BSA), and human serum albumin (HSA) were purchased from sigma-aldrich. Pyroglutamyl aminopeptidase I (PGP-1) was the production of Maibo Pharmaceutical Co., Ltd.

NMR spectra of the synthesized compounds and isolated natural compounds were acquired using a Bruker-500 and 600 with tetramethylsilane (TMS) as the internal standard (Bruker, USA). High resolution mass spectral (HRMS) was measured using a G6224A TOF-MS. HPLC analysis was performed on a Dionex UltiMate 3000 equipped with a DAD detector and a C18 silica gel column (Thermo Scientific, USA). Natural compounds were purified using pre-HPLC manufactured by Agel Technology, which

contained an YMC (250 mm × 10 mm) column packed with C18 (5 μm) silica gel, followed using a UV detector. A constant temperature incubator shaker (HZQ-C) was obtained from Harbin Donglian Electronic Technology Development Co., LtD (China). A confocal laser scanning microscope was manufactured by Leica (German). Fluorescence spectra and fluorescence intensity were obtained using a BioTek Synergy H1 microplate reader (BioTek, USA). The fluorescence imaging for the high throughput screening of inhibitors was recorded using an Amersham Typhoon RGB (GE, USA).

*2.2. Synthesis of the fluorescent probe **DDPA***

The fluorescent probe **DDPA** was synthesized according to the route as shown in Scheme S1 (Scheme S1).

*2.2.1. Synthesis of **DDAN***

Compound **DDAN** was prepared according to our previous report.[36] ^{1}H NMR (500 MHz, DMSO-d_6) δ_H 7.70 (s, 1H), 7.37 (d, J = 8.7 Hz, 1H), 7.22 (s, 2H), 6.87 (d, J = 2.3 Hz, 1H), 6.67 (dd, J = 8.7, 2.3 Hz, 1H), 1.77 (s, 6H).

HATU (760.4 mg, 2.0 mmol) and DIEA (258.6 mg, 2.0 mmol) was added into a solution of N-(tert-Butoxycarbonyl)-L-pyroglutamic acid (458.5 mg, 2.0 mmol) in anhydrous DMF (15 mL), and the mixture was stirred for 30 min at 0 °C. Then, a solution of **DDAN** (459.0 mg, 1.5 mmol) in anhydrous DMF (12 mL) was added, and the mixture was stirred at room temperature (RT) for further 12 h. Then the mixture was diluted with CH_2Cl_2, and washed three times with water. The organic phase was dried over $MgSO_4$ and evaporated under reduced pressure, and the residues were purified over a silica column with CH_2Cl_2/MeOH (30/1 *v/v*) to afford compound **DDPA-Boc** as an orange solid (87.6 mg, yield: 11.3 %). ^{1}H NMR (500 MHz, $CDCl_3$) δ_H 9.16 (s, 1H), 8.03 (d, J = 1.8 Hz, 1H), 7.70 – 7.62 (m, 2H), 7.59 (d, J = 8.6 Hz, 1H), 4.75 (dd, J = 8.7, 4.9 Hz, 1H), 2.76 (dt, J = 17.4, 8.8 Hz, 1H), 2.63 – 2.56 (m, 1H), 2.47 – 2.32 (m, 2H), 1.88 (d, J = 7.3 Hz, 6H), 1.48 (s, 9H). ^{13}C NMR (125 MHz, $CDCl_3$) δ_C 174.71, 173.28, 169.49, 149.94, 148.73, 141.73, 140.94, 139.63, 139.49, 137.79, 136.91, 134.99, 132.94, 119.43, 117.93, 84.69, 61.80, 39.21, 31.98, 28.04, 26.70, 26.68, 21.57. HRMS (ESI positive) calcd for $[M+H]^+$ 518.1244, found 518.1248.

*2.2.2. Synthesis of compound **DDPA***

Trifluoroacetic acid (3 mL) was added into a solution of **DDPA-Boc** (51.7 mg, 0.1 mmol) in CH_2Cl_2 (8 mL), and the mixture was stirred for 8 h at RT. After removing the solvent, the residues were purified over a silica column with CH_2Cl_2/MeOH (10/1 *v/v*) to afford **DDPA** as an orange solid (34.7 mg, yield: 83.2 %). ^{1}H NMR (500 MHz, MeOD) δ_H 8.05 (s, 1H), 7.71 (s, 1H), 7.64 (d, J = 11.6 Hz, 2H), 4.41 – 4.35 (m, 1H), 2.61 – 2.45 (m, 2H), 2.38 (dd, J = 16.2, 10.2 Hz, 1H), 2.22 (s, 1H), 1.92 (s, 6H). ^{13}C NMR (100 MHz, MeOD) δ_C 180.20, 173.01, 172.13, 148.59, 142.32, 141.11, 139.63, 139.27, 137.42, 136.45, 134.43, 132.50, 118.91, 117.41, 57.52, 39.02, 29.08, 25.64, 25.36. HRMS (ESI negative) calcd for $[M-H]^-$ 416.0574, found 416.0569.

*2.3. Enzymatic hydrolysis of **DDPA** mediated by PGP-1*

The enzymatic hydrolysis of **DDPA** mediated by PGP-1 was performed in phosphate buffer (PB, pH 7.4) containing K_2HPO_4 and KH_2PO_4 (K^+ 100 mM). 200 μL PB containing PGP-1 (0.05 μg/mL) and **DDPA** (10 μM) were shaken under constant temperature (37 °C) for 1h. Then, 100 μL acetonitrile was used to terminate the enzymatic reaction before the removing of denatured protein by centrifugation (20000 *g*, 10 min). The fluorescence spectra (λ_{ex} 600/λ_{em} 670 nm) of the supernatant were evaluated using a microplate reader.

In addition, the fluorescence intensity during a series enzymatic hydrolyses with **DDPA** (10 μM) were monitored with the addition of PGP-1 at different concentrations (0, 0.002, 0.005, 0.01, 0.02, 0.03, 0.04, 0.05, 0.06 μg/mL).

The selectivity of **DDPA** toward PGP-1 was evaluated through the co-incubation of **DDPA** and various biological enzymes CYP4F2, CE2, CE1c, CE1b, PGP-1, PGA, BSA, HSA, GGT, APN, LAP and lipase (0.05 μg/mL). The effect on the fluorescence intensity of **DDPA** and the enzymatic hydrolysis of **DDPA** was evaluated using various species, including ions (Mn^{2+}, Ca^{2+}, Mg^{2+}, Ni^{2+}, Zn^{2+}, Sn^{4+}, Fe^{3+}, Ba^{2+}, Cr^{6+}, K^+, Cu^{2+}, Na^+ (200 μM), amino acids (Ser, Trp, Tyr, Gly, Gys, Arg, Lys, Gln, GSH, 10 μM), and glucose (10 μM).

2.4. Investigation of the inhibitory effects of natural products on PGP-1

The high throughput screening for PGP-1 inhibitors were performed in 96-well plates by the co-incubation about PGP-1 (0.05 μg/mL), **DDPA** (10 μM) and various herb

extracts (1 μg/mL) with the same enzymatic reaction conditions as mentioned above. The herbs used are listed in Table S1. Then, the plate was subjected to fluorescence imaging (λ_{ex} = 635 nm, λ_{em} = 670 ± 15 nm) using an Amersham Typhoon RGB. According to the fluorescence intensity of individual wells, the inhibitory effect of each herb was determined. The inhibitory effect of isolated compounds was evaluated using the same protocol.

2.5. Isolation and spectroscopic data of isolated natural compounds from P. corylifolia as PGP-1 inhibitors

The powdered *P. corylifolia* (100 g) was extracted using an ultrasonic method in ethanol three times. After evaporation of ethanol under reduced pressure, the residue was analyzed using HPLC (ODS column), with CH_3OH-H_2O (0.05% TFA, *v/v*) as the mobile phase (gradient change 10% -100% CH_3OH 0-30 min; 100%-100% CH_3OH 10 min; flow rate 0.8 mL/min). Then, the ethanolic extract of *P. corylifolia* was separated by an automatic purification system equipped with a RP-C18 column. The chromatographic method used 10%-100% CH_3OH, 0-60 min, flow rate 8 mL/min. 11 fractions were collected for evaluation as PGP-1 inhibitors. Fractions 6, 8, and 11 were determined to be bioactive, andwere therefore isolated to facilitate identificated. Finally, the ^1H, ^{13}C NMR, and HR-MS spectral data for fractions 6, 8, and 11were acquired to elucidate the structures by comparison with the previously reported data. The HPLC chromatographic method for isobavachalcone was set as 50% CH_3CN-50% H_2O (0.05% TFA, *v/v*), flow rate 0.8 mL/min. The HPLC chromatographic method for corylinin and bakuchiol was set as 60% CH_3CN-40% H_2O (0.05% TFA, *v/v*), flow rate 0.8 mL/min.

Isobavachalcone. ^1H NMR (600 MHz, DMSO-d_6) δ_H 14.00 (1H, s), 10.57 (1H, s), 10.12 (1H, s), 8.04 (1H, d, J = 9.0 Hz), 7.75 (1H, m), 6.84 (2H, d, J = 9.0 Hz), 6.47 (1H, d, J = 8.4 Hz), 5.18 (1H, m), 3.23 (2H, d, J = 7.2 Hz), 1.73 (3H, s), 1.62 (3H, s). ^{13}C NMR (150 MHz, DMSO-d_6) δ_C 191.76, 163.53, 162.27, 160.24, 144.12, 131.19, 130.45, 129.81, 125.77, 122.36, 117.37, 115.84, 114.44, 112.70, 107.30, 25.48, 21.26, 17.71. HR-MS (+ESI) *m/z* 325.1424 $[M+H]^+$, calcd for $C_{20}H_{21}O_4$ 325.1434.

Corylinin. ^1H NMR (600 MHz, DMSO-d_6) δ_H 10.76 (1H, brs), 9.44 (1H, s), 8.24 (1H, s), 7.95 (1H, d, J = 9.0 Hz), 7.23 (1H, d, J = 2.4 Hz), 7.18 (1H, dd, J = 8.4, 2.4

Hz), 6.93 (1H, dd, *J* = 9.0, 2.4 Hz), 6.85 (1H, d, *J* = 2.4 Hz), 6.82 (1H, d, *J* = 9.0 Hz), 5.31 (1H, m), 5.07 (1H, m), 3.25 (1H, d, *J* = 7.2 Hz), 2.05 (2H, m), 1.98 (2H, m), 1.68 (3H, s), 1.56 (3H, brs), 1.53 (3H, s). ^{13}C NMR (150 MHz, DMSO-d_6) δ_C 174.70, 162.47, 157.41, 154.80, 152.68, 134.95, 130.68, 129.98, 127.34, 127.27, 127.04, 124.07, 123.81, 122.59, 122.52, 116.64, 115.08, 114.46, 102.06, 27.90, 26.11, 25.38, 17.54, 15.88. HR-MS (+ESI) *m/z* 391.1904 $[M+H]^+$, calcd for $C_{25}H_{27}O_4$ 391.1904.

Bakuchiol. ^{1}H NMR (600 MHz, DMSO-d_6) δ_H 9.38 (1H, s), 7.21 (2H, d, *J* = 8.4 Hz), 6.69 (2H, d, *J* = 8.4 Hz), 6.19 (1H, d, *J* =16.8 Hz), 6.04 (1H, d, *J* =16.8 Hz), 5.88 (1H, dd, *J* =17.4, 10.8 Hz), 5.10 (1H, m), 5.17 (1H, dd, *J* =10.8, 1.2 Hz), 4.98 (1H, dd, *J* =17.4, 1.2 Hz), 1.89 (1H, m), 1.63 (3H, s), 1.53 (3H, s), 1.43 (2H, m), 1.15 (3H, s). ^{13}C NMR (150 MHz, DMSO-d_6) δ_C 156.63, 145.90, 134.00, 130.50, 128.31, 127.14, 126.48, 124.69, 115.32, 111.80, 42.07, 40.92, 25.46, 23.00, 22.84, 17.46. HR-MS (+ESI) *m/z* 257.1929 $[M+H]^+$, calcd for $C_{18}H_{25}O$ 257.1900.

*2.6. Identification of target intestinal microbiota from human feces using **DDPA***

The human stools of healthy subject were collected from Dalian Medical University. The fresh stools were dispersed in sterile water immediately, which was then cultured on nutrient broth agar medium (NB) until the formation of obvious colonies (37 ºC, 48 h). When the bacterial colonies were observed on the agar plates, **DDPA** was dropped onto the bacterial colonies for a co-incubation of 5 h. Then, fluorescence images of the agar plates were obtained using an Amersham Typhoon RGB (λ_{ex} 635 nm, λ_{em} 670 ± 15 nm). For the bacterial colonies with strong fluorescence intensity, a further purification was performed on the NB culture. The isolated bacteria strains were identified by 16s rDNA sequence. The RT-PCR primers were as follows.

1510 R: 5'-ACGGYTACCTTGTTACGACTT-3'

7F: 5'-AGAGTTTGATYMTGGCTCAG-3'

*2.7. Fluorescence imaging of B. velezensis FZB42 cells using **DDPA***

B. velezensis FZB42 was cultured in NB medium to get enough cells with OD_{600} values at 0.7 - 0.8. The medium was removed by centrifugation (5000 rpm, 10 min). The bacterial cells were washed two times using PB (1 mL) and suspended into PB (1 mL) following pre-incubation for 3 min at 37 °C. Then,

DDPA (50 μM) was added into the bacterial suspension for incubation at 37 °C (6 h). For the inhibitory experiments, inhibitors (100 μM) were added into the bacterial suspension together with the fluorescent probe. After incubation, the clear bacterial cells were prepared by a washing procedure using PB and centrifugation (5000 rpm). The bacterial cells were resuspended in 30 μL PB for fluorescence imaging experiments. The bacterial suspension was dropped onto a glass slide, which was subjected to confocal laser scanning microscopy to obtain fluorescence images (λ_{ex} = 633 nm, λ_{em} = 645 - 690 nm).

3. Results and discussion

3.1. Development of a fluorescent probe for PGP-1

It is well known that PGP-1 hydrolase could hydrolyze the amide bond located on the L-pyroglutamate (L-pGlu) residue at the amino terminus of proteins and peptides. Therefore, guided by the biological function of PGP-1, pyroglutamic acid was attached to **DDAN** using an amide bond as a recognition unit, affording the designed fluorescent probe **DDPA**, which should be hydrolyzed by PGP-1, to generate the NIR fluorescent molecule **DDAN** (Fig. 1a). With **DDPA** in hand, the enzymatic reaction with PGP-1 was monitored using high performance liquid chromatography (HPLC). From which, **DDAN** was detected in the PGP-1 enzymatic reaction (Fig. S1). On enzymatic reaction, the absorbance spectra exhibited a large red shift from 474 nm to 600 nm, and a strong fluorescence intensity was observed at 670 nm, which confirms the potential of **DDPA** as an off-on fluorescent probe for the detection of PGP-1 (Fig. 1b).

The fluorescence responses of **DDPA** toward PGP-1 under various conditions were then evaluated to determine a suitable activity assay system for PGP-1. As shown in Fig. 2a, a series fluorescence curves were obtained for the incubation of **DDPA** and PGP-1 at different concentrations. Furthermore, an excellent linear relationship was observed between the fluorescence intensity at 670 nm and PGP-1 concentrations (Fig. 2b), which suggested the quantitative application of **DDPA** for PGP-1 analysis. For fluorescent probes, the selectivity of **DDPA** toward PGP-1 is an important parameter. As such, the fluorescence responses of

DDPA toward various biological enzymes, amino acids, and ions were evaluated. Only a weak fluorescence signal was observed for the co-incubation of **DDPA** with biological enzymes, and in particular the aminopeptidases leucine aminopeptidase (LAP), aminopeptidase N (APN), γ-glutamyl-transferase (GGT) (Fig. 2c). In addition, amino acids and ions did not influence on the fluorescence signal of **DDPA** (Fig. S3). Finally, the kinetics of the hydrolysis of **DDPA** mediated by PGP-1 was determined using the Hill model (Fig. 2d), with the kinetic parameters V_{max} = 2.38 μmol/min/mg, K_m = 8.305 μmol. Therefore, **DDPA** was confirmed as a suitable enzyme-activated NIR fluorescent probe for PGP-1, with high sensitivity and selectivity.

*3.2. High throughput screening of PGP-1 inhibitors using **DDPA***

Using **DDPA** as the fluorescent probe, a visual high throughput screening (HTS) system was established to assay PGP-1 activity and identify inhibitors. In a 96-well plate, 54 medical herb extractions were evaluated for their inhibitory effect on PGP-1 (Table S1). After the fluorescence imaging of the plate, the fluorescence intensity of each well visually indicated the inhibitory effect (Fig. 3a). No. 9 well displayed the weakest fluorescence intensity, suggesting the strongest inhibitory effect for *P. corylifolia* against the hydrolase activity of PGP-1, which was also confirmed by the fluorescence intensity measurements (Fig. S4). We then set out to determine the bioactive chemical constituent of *P. corylifolia* for PGP-1 exhibiting the inhibitory effect using widely available methods, including inhibitory evaluation, chromatography, and spectroscopic analysis. Firstly, the extract of *P. corylifolia* was subjected to HPLC separation, 11 fractions were collected for evaluation of the inhibitory effect (Fig. 3b). On the basis of high throughput screening established using **DDPA**, fractions 6, 8, and 11 were determined to be the most bioactive constituents (Fig. 3c). After further separation by preparative HPLC, three bioactive compounds were purified and their ^{1}H NMR, ^{13}C NMR, ESI-MS data were acquired.

The spectroscopic data of isolated compound **BGZ-6** from fraction 6 were indicative of a chalcone skeleton, possessing three hydroxyl groups, and an

isopentenyl moiety. The spectroscopic data of **BGZ-6** were identical with the known compound isobavachalcone from *P. corylifolia*.[37] On the basis of the NMR and HR-MS data obtained for **BGZ-8** from fraction 11, an isoflavone skeleton was deduced, together with two hydroxyl groups and one geranyl group. The spectroscopic data of **BGZ-8** corelated with corylinin, which is a previously reported compound from *P. corylifolia*.[38] The spectroscopic data of isolated compound (**BGZ-11**) from fraction 11, indicated a di-substituted aromatic ring, a terminal olefinic bond, a trans double bond, and three methyl groups. The HR-MS together with NMR data confirmed the molecular formula to be $C_{18}H_{24}O$ for **BGZ-11**. These spectroscopic data for **BGZ-11** were consistent with bakuchiol, a known compound from *P. corylifolia*.[37]

In summary the spectroscopic data facilitated identification of the isolated compounds as isobavachalcone, corylinin, and bakuchiol (Fig. 3d), which are known compounds from *P. corylifolia*. Using an activity assay for PGP-1, significant inhibitory effects were determined for isobavachalcone (IC_{50} 1.79 μM), corylinin (IC_{50} 1.43 μM), and bakuchiol (IC_{50} 7.95 μM). Our preliminary structural analysis indicated that flavone analogues exhibited stronger inhibitory effects towards PGP-1. Significantly, this is the first report concerning the inhibitory effects of extracted compounds from *P. corylifolia* for PGP-1, and indicate the potential of these extracts for interfering with bacterial metabolism.

3.3. Visual identification of intestinal bacteria with active PGP-1

Intestinal bacteria exhibiting PGP-1 expression are important for the metabolism of endogenous and exogenous biological peptides. Therefore, the identification of these target bacteria is essential for a functional investigation of intestinal microbiota. Therefore, a human fresh stool was diluted with sterile water, and coated on nutrient broth agar plates for bacterial cultivation. When the bacterial colonies were observed, **DDPA** was sprayed on these colonies for the sensing of endogenous PGP-1. Subsequently, the fluorescence images of these plates were obtained using a fluorescence imager. As shown in Fig. 4b, the colonies with strong fluorescence intensity were picked for further purification

of target bacteria. Finally, eight intestinal bacterial strains were isolated and identified as (1) *Klebsiella pneumoniae* DSM 30104, (2) *Klebsiella pneumoniae* subsp. rhinoscleromatis strain R-70, (3) *Klebsiella variicola* F2R9, (4) *Klebsiella aerogenes* NBRC 13534, (5) *Shigella flexneri* ATCC 29903, (6) *Escherichia fergusonii* ATCC 35469, (7) *Shigella sonnei* CECT 4887, and (8) *Bacillus velezensis* FZB42. Then, the isolated bacterial strains were cultured on agar plates respectively. **DDPA** was dropped onto these bacterial colonies for the visual sensing of endogenous PGP-1. As shown in Fig. 4c, the fluorescence images obtained for these bacterial plates indicated the expression of active PGP-1 for eight bacterial strains. Furthermore, **DDPA** was incubated with *B. velezensis* FZB42 solution, which was then subjected to HPLC analysis. As expected, the fluorophore molecule **DDAN** as the hydrolysis product was detected, confirming the existence of active PGP-1 (Fig. S5). In summary, the visual sensing of endogenous PGP-1 in bacterial colonies using **DDPA**, facilitated the efficient identification and culture of bacterial strains from human feces.

Additionally, *B. velezensis* FZB42 was incubated with **DDPA** and imaged using a confocal laser scanning microscope. A fluorescence image was obtained with strong fluorescence for the bacterial cells in comparison with the blank group (Fig. 5a, 5b). While, when the inhibitor bakuchiol from *P. corylifolia* and the previously reported inhibitor alantolactone were used to inhibit the hydrolysis of **DDPA** by *B. velezensis* FZB42, a weak fluorescence signal was measured for these bacterial cells (Fig. 5c and 5d). Thus, **DDPA** can be used for the visual sensing of endogenous PGP-1 activity in bacteria.

4. Conclusions

Intestinal bacteria are associated with many aspects of human health and diseases. PGP-1 expressed by intestinal bacteria is involved in the metabolism of various biological peptides possessing L-pGlu residues. In this study, an enzymatic activatable NIR fluorescent probe (**DDPA**) was developed for the real time sensing of PGP-1. Using **DDPA**, a high throughput screening system for

PGP-1 activity was established, which guided the isolation of three natural inhibitors from *Psoralea corylifolia*. In addition, eight intestinal bacterial strains were identified and cultivated from human feces under the guidance of the visual sensing of bacterial PGP-1 by **DDPA**. In summary, bacterial PGP-1 was visually detected by **DDPA**, which was used to identify natural inhibitors and intestinal bacteria successfully.

CRediT authorship contribution statement

Chao Wang: Investigation, and writing. **Zhenhao Tian:** Synthesis. **Ming Zhang:** Bacteria culture. **Ying Deng:** Fluorescence imaging. **Xiangge Tian:** Validation. **Lei Feng:** NMR spectra, and editing. **Jingnan Cui:** Validation. **Tony D. James:** Writing, review & editing, and funding. **Xiaochi Ma:** Design, and funding.

Declaration of competing interest

The authors declare that they have no known competing financial interests or personal relationships that could have appeared to influence the work reported in this paper.

Acknowledgments

This work was supported financially by National Natural Science Foundation of China (No. 81930112), Dalian Science and Technology Leading Talents Project (2019RD15), Liaoning Provincial Natural Science Foundation (20180550761 and 2019-BS-056), Liaoning Revitalization Talents Program (XLYC1907017), State Key Laboratory of Fine Chemicals, Dalian University of Technology (KF1912), High-level Talents of Dalian (2020RQ076, 2020RJ09) and the Open Research Fund of the School of Chemistry and Chemical Engineering, Henan Normal University (2020ZD01 and 2021YB07). T.D.J. wishes to thank the Royal Society for a Wolfson Research Merit Award.

Appendix A. Supplementary data

Supplementary data to this article can be found online.

References

[1] S.C. Forster, N. Kumar, B.O. Anonye, A. Almeida, E. Viciani, M.D. Stares, M. Dunn, T.T. Mkandawire, A. Zhu, Y. Shao, L.J. Pike, T. Louie, H.P. Browne, A.L. Mitchell, B.A. Neville, R.D. Finn, T.D. Lawley, A human gut bacterial genome and culture collection for improved metagenomic analyses, Nat. Biotechnol. 37(2) (2019) 186-192.

[2] J.C. Lagier, S. Khelaifia, M.T. Alou, S. Ndongo, N. Dione, P. Hugon, A. Caputo, F. Cadoret, S.I. Traore, E.H. Seck, G. Dubourg, G. Durand, G. Mourembou, E. Guilhot, A. Togo, S. Bellali, D. Bachar, N. Cassir, F. Bittar, J. Delerce, M. Mailhe, D. Ricaboni, M. Bilen, N.P. Dangui Nieko, N.M. Dia Badiane, C. Valles, D. Mouelhi, K. Diop, M. Million, D. Musso, J. Abrahao, E.I. Azhar, F. Bibi, M. Yasir, A. Diallo, C. Sokhna, F. Djossou, V. Vitton, C. Robert, J.M. Rolain, B. La Scola, P.E. Fournier, A. Levasseur, D. Raoult, Culture of previously uncultured members of the human gut microbiota by culturomics, Nat. Microbiol. 1 (2016) 16203.

[3] Y. Zou, W. Xue, G. Luo, Z. Deng, P. Qin, R. Guo, H. Sun, Y. Xia, S. Liang, Y. Dai, D. Wan, R. Jiang, L. Su, Q. Feng, Z. Jie, T. Guo, Z. Xia, C. Liu, J. Yu, Y. Lin, S. Tang, G. Huo, X. Xu, Y. Hou, X. Liu, J. Wang, H. Yang, K. Kristiansen, J. Li, H. Jia, L. Xiao, 1,520 reference genomes from cultivated human gut bacteria enable functional microbiome analyses, Nat. Biotechnol. 37(2) (2019) 179-185.

[4] J. Halfvarson, C.J. Brislawn, R. Lamendella, Y. Vazquez-Baeza, W.A. Walters, L.M. Bramer, M. D'Amato, F. Bonfiglio, D. McDonald, A. Gonzalez, E.E. McClure, M.F. Dunklebarger, R. Knight, J.K. Jansson, Dynamics of the human gut microbiome in inflammatory bowel disease, Nat. Microbiol. 2 (2017) 17004.

[5] I. Dickson, Gut microbiota: Diagnosing IBD with the gut microbiome, Nat Rev Gastroenterol. Hepatol. 14(4) (2017) 195.

[6] H. Sokol, V. Leducq, H. Aschard, H.P. Pham, S. Jegou, C. Landman, D. Cohen, G. Liguori, A. Bourrier, I. Nion-Larmurier, J. Cosnes, P. Seksik, P. Langella, D. Skurnik, M.L. Richard, L. Beaugerie, Fungal microbiota dysbiosis in IBD, Gut 66(6) (2017) 1039-1048.

[7] I. Nemet, P.P. Saha, N. Gupta, W. Zhu, K.A. Romano, S.M. Skye, T. Cajka, M.L. Mohan, L. Li, Y. Wu, M. Funabashi, A.E. Ramer-Tait, S.V. Naga Prasad, O. Fiehn, F.E. Rey, W.H.W. Tang, M.A. Fischbach, J.A. DiDonato, S.L. Hazen, A Cardiovascular Disease-Linked Gut Microbial Metabolite Acts via Adrenergic Receptors, Cell 180(5) (2020) 862-877 e22.

[8] V. Maini Rekdal, E.N. Bess, J.E. Bisanz, P.J. Turnbaugh, E.P. Balskus, Discovery and inhibition of an interspecies gut bacterial pathway for Levodopa metabolism, Science 364(6445) (2019).

[9] B. Javdan, J.G. Lopez, P. Chankhamjon, Y.J. Lee, R. Hull, Q. Wu, X. Wang, S. Chatterjee, M.S. Donia, Personalized Mapping of Drug Metabolism by the Human Gut Microbiome, Cell 181(7) (2020) 1661-1679 e22.

[10] M. Zimmermann, M. Zimmermann-Kogadeeva, R. Wegmann, A.L. Goodman, Mapping human microbiome drug metabolism by gut bacteria and their genes, Nature 570(7762) (2019) 462-467.

[11] T. Gonzales, J. Robert-Baudouy, Bacterial aminopeptidases: properties and functions, FEMS Microbiol. Rev. 18(4) (1996) 319-344.

[12] M. Cellier, A.L. James, S. Orenga, J.D. Perry, A.K. Rasul, S.N. Robinson, S.P. Stanforth, Novel chromogenic aminopeptidase substrates for the detection and identification of clinically important microorganisms, Bioorg. Med. Chem. 22(19) (2014) 5249-5269.

[13] P. Kutzer, C. Schulze, A. Engelhardt, L.H. Wieler, M. Nordhoff, Helcococcus ovis, an emerging pathogen in bovine valvular endocarditis, J. Clin. Microbiol. 46(10) (2008) 3291-3295.

[14] K. Fujiwara, R. Kobayashi, D. Tsuru, The substrate specificity of pyrrolidone carboxylyl peptidase from Bacillus amyloliquefaciens, Biochim. Biophys. Acta 570(1) (1979) 140-148.

[15] Y. Odagaki, A. Hayashi, K. Okada, K. Hirotsu, T. Kabashima, K. Ito, T. Yoshimoto, D. Tsuru, M. Sato, J. Clardy, The crystal structure of pyroglutamyl peptidase I from Bacillus amyloliquefaciens reveals a new structure for a cysteine protease, Structure 7(4) (1999) 399-411.

[16] J. Irazusta, J. Gil, F. Ruiz, N. Agirregoitia, L. Casis, P.F. Silveira, Effect of the disruption of body fluid balance on pyroglutamyl aminopeptidase (Type-1) in rat brain structures, Neuropeptides 36(5) (2002) 333-340.

[17] A.C. Awade, P. Cleuziat, T. Gonzales, J. Robert-Baudouy, Pyrrolidone carboxyl peptidase (Pcp): an enzyme that removes pyroglutamic acid (pGlu) from pGlu-peptides and pGlu-proteins, Proteins 20(1) (1994) 34-51.

[18] K. Abe, K. Fukuda, T. Tokui, Marginal involvement of pyroglutamyl aminopeptidase I in metabolism of thyrotropin-releasing hormone in rat brain, Biol. Pharm. Bull. 27(8) (2004) 1197-1201.

[19] K. Bauer, P. Nowak, Characterization of a thyroliberin-degrading serum enzyme catalyzing the hydrolysis of thyroliberin at the pyroglutamyl-histidine bond, Eur. J. Biochem. 99(2) (1979) 239-246.

[20] T. Cao, L. Zhang, H. Ma, L. Zheng, Y. Cao, J. Wang, Y. Yang, J. Zhang, W. Qin, Y. Liu, Near-infrared ratio fluorescent sensor for the study of PGP-1 in inflammation and tumor mice, Sens. Actuators B: Chemical 338 (2021) 129841.

[21] Q. Gong, L. Li, X. Wu, H. Ma, Pyroglutamate aminopeptidase 1 may be an indicator of cellular inflammatory response as revealed using a sensitive long-wavelength fluorescent probe, Chem. Sci. 7(7) (2016) 4694-4697.

[22] Q. Gong, R. Zou, J. Xing, L. Xiang, R. Zhang, A. Wu, A Ultrasensitive Near-Infrared Fluorescent Probe Reveals Pyroglutamate Aminopeptidase 1 Can Be a New Inflammatory Cytokine, Adv. Sci. (Weinh) 5(4) (2018) 1700664.

[23] T. Cao, L. Zhang, L. Zheng, J. Qian, A. Iqbal, K. Iqbal, W. Qin, Y. Liu, A ratiometric fluorescent sensor for rapid detection of the pyroglutamate aminopeptidase-1 in mouse tumors, J. Mater. Chem. B 9(22) (2021) 4546-4554.

[24] D. Chen, W. Qin, H. Fang, L. Wang, B. Peng, L. Li, W. Huang, Recent progress in two-photon small molecule fluorescent probes for enzymes, Chin. Chem. Let. 30(10) (2019) 1738-1744.

[25] L. Feng, P. Li, J. Hou, Y.L. Cui, X.G. Tian, Z.L. Yu, J.N. Cui, C. Wang, X.K. Huo, J. Ning, X.C. Ma, Identification and Isolation of Glucosytransferases (GT) Expressed Fungi Using a Two-Photon Ratiometric Fluorescent Probe Activated by GT, Anal. Chem. 90(22) (2018) 13341-13347.

[26] L. Feng, Z. Tian, M. Zhang, X. He, X. Tian, Z. Yu, X. Ma, C. Wang, Real-time identification of gut microbiota with aminopeptidase N using an activable NIR fluorescent probe, Chin. Chem. Let. 10.1016/j.cclet.2021.03.056 (2021).

[27] L. Feng, Q. Yan, B. Zhang, X. Tian, C. Wang, Z. Yu, J. Cui, D. Guo, X. Ma, T.D. James, Ratiometric fluorescent probe for sensing Streptococcus mutans glucosyltransferase, a key factor in the formation of dental caries, Chem. Commun. (Camb) 55(24) (2019) 3548-3551.

[28] X. He, L. Li, Y. Fang, W. Shi, X. Li, H. Ma, In vivo imaging of leucine aminopeptidase activity in drug-induced liver injury and liver cancer via a near-infrared fluorescent probe, Chem. Sci. 8(5) (2017) 3479-3483.

[29] J. Li, L. Chen, W. Wu, W. Zhang, Z. Ma, Y. Cheng, L. Du, M. Li, Discovery of bioluminogenic probes for aminopeptidase N imaging, Anal. Chem. 86(5) (2014) 2747-51.

[30] L. Li, L. Feng, M. Zhang, X. He, S. Luan, C. Wang, T.D. James, H. Zhang, H. Huang, X. Ma, Visualization of penicillin G acylase in bacteria and high-throughput screening of natural inhibitors using a ratiometric fluorescent probe, Chem. Commun. (Camb) 56(34) (2020) 4640-4643.

[31] T. Liu, Q.L. Yan, L. Feng, X.C. Ma, X.G. Tian, Z.L. Yu, J. Ning, X.K. Huo, C.P. Sun, C. Wang, J.N. Cui, Isolation of gamma-Glutamyl-Transferase Rich-Bacteria from Mouse Gut by a Near-Infrared Fluorescent Probe with Large Stokes Shift, Anal. Chem. 90(16) (2018) 9921-9928.

[32] Z. Tian, Q. Yan, L. Feng, S. Deng, C. Wang, J. Cui, C. Wang, Z. Zhang, T.D. James, X. Ma, A far-red fluorescent probe for sensing laccase in fungi and its application in developing an effective biocatalyst for the biosynthesis of antituberculous dicoumarin, Chem. Commun. (Camb) 55(27) (2019) 3951-3954.

[33] X. Tian, T. Liu, Y. Ma, J. Gao, L. Feng, J. Cui, T.D. James, X. Ma, A Molecular-Splicing Strategy for Constructing a Near-Infrared Fluorescent Probe for UDP-Glucuronosyltransferase 1A1, Angew Chem Int Ed Engl 10.1002/anie.202109479 (2021).

[34] H. Li, D. Kim, Q. Yao, H. Ge, J. Chung, J. Fan, J. Wang, X. Peng, J. Yoon, Activity-Based NIR Enzyme Fluorescent Probes for the Diagnosis of Tumors and Image-Guided Surgery, Angew Chem Int Ed Engl 60(32) (2021) 17268-17289.

[35] J. Ning, T. Liu, P. Dong, W. Wang, G. Ge, B. Wang, Z. Yu, L. Shi, X. Tian, X. Huo, L. Feng, C. Wang, C. Sun, J. Cui, T.D. James, X. Ma, Molecular Design Strategy to Construct the Near-Infrared Fluorescent Probe for Selectively Sensing Human Cytochrome P450 2J2, J. Am. Chem. Soc. 141(2) (2019) 1126-1134.

[36] L.F. Zhenhao Tian, Lu Li, Xiangge Tian, Jingnan Cui, Houli Zhang, Chao Wang, Shanshan Huang, Baojing Zhang, Xiaochi Ma, Visualized characterization of bacterial penicillin G acylase for the hydrolysis of β-lactams using an activatable NIR fluorescent probe, Sens. Actuators: B. Chemical 210 (2020) 127872.

[37] S.W. Lee, B.R. Yun, M.H. Kim, C.S. Park, W.S. Lee, H.M. Oh, M.C. Rho, Phenolic compounds isolated from Psoralea corylifolia inhibit IL-6-induced STAT3 activation, Planta Med. 78(9) (2012) 903-906.

[38] B. Ruan, L.Y. Kong, Y. Takaya, M. Niwa, Studies on the chemical constituents of Psoralea corylifolia L, J. Asian. Nat. Prod. Res. 9(1) (2007) 41-44.

Figures

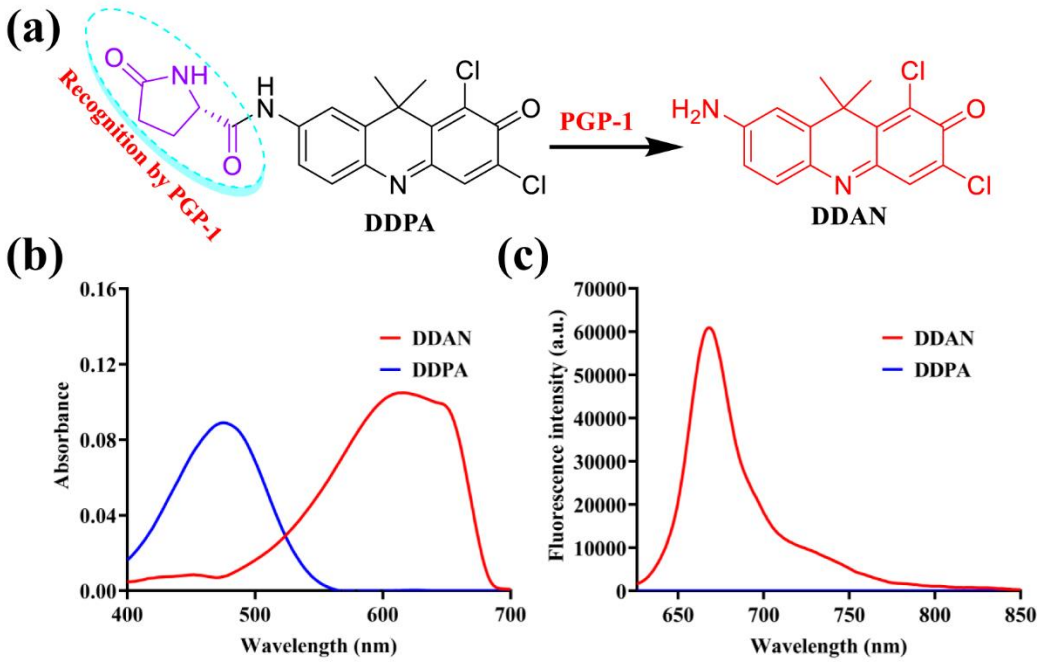

Fig. 1. (a) Enzymatic hydrolysis of **DDPA** by PGP-1. (b) The absorbance spectra of **DDAN** and **DDPA**. (c) The fluorescence spectra of **DDAN** and **DDPA**.

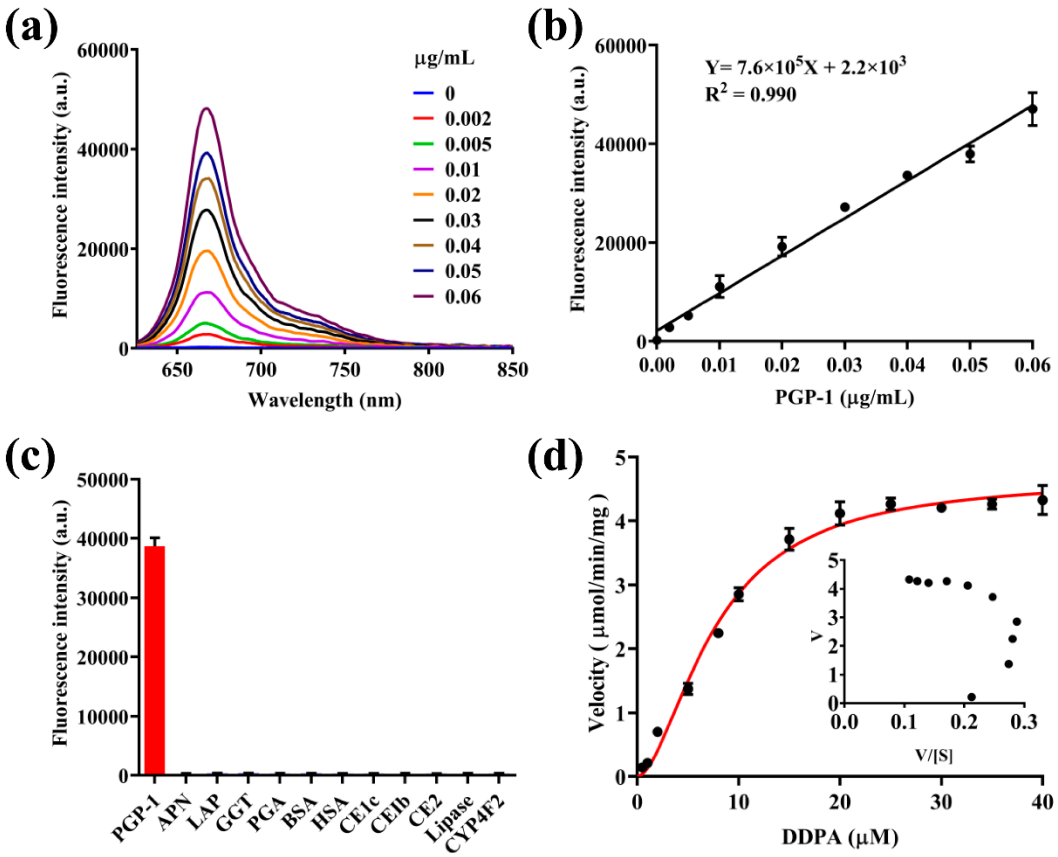

Fig. 2. (a) Fluorescence responses of **DDPA** toward PGP-1 at different concentrations. (b) Relationship between the fluorescence intensity at 670 nm and PGP-1 at different concentrations. (c) Fluorescence responses of **DDPA** toward various biological enzymes. (d) Enzymatic kinetics for the hydrolysis of **DDPA** mediated by PGP-1.

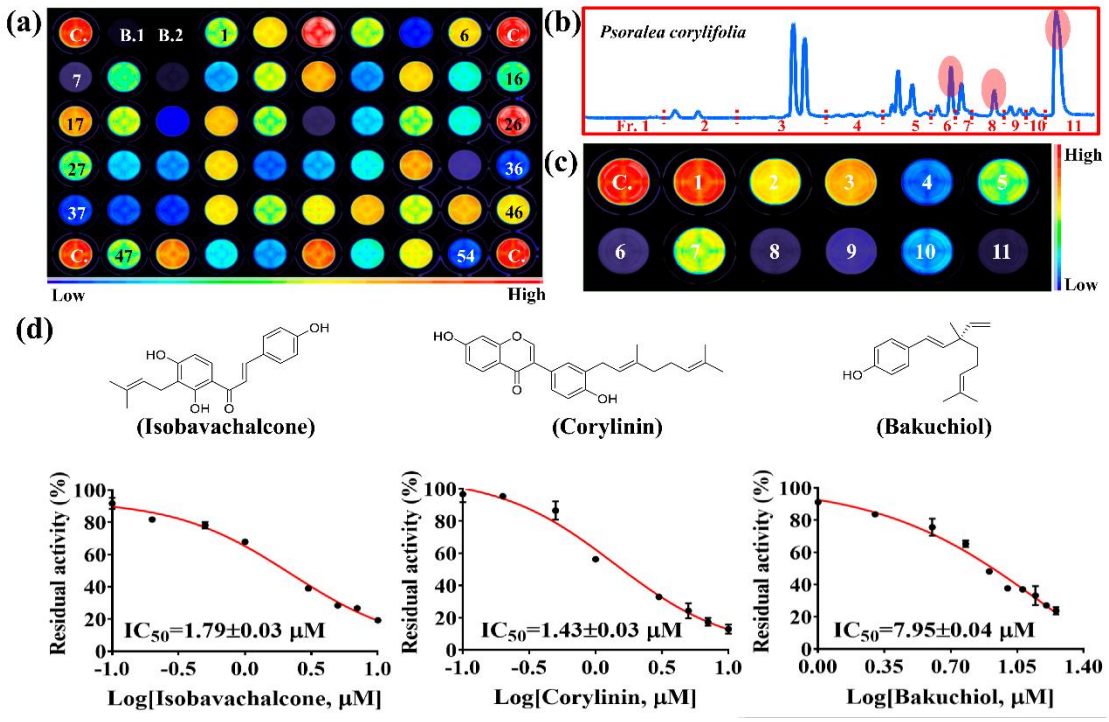

Fig. 3. The identification of natural inhibitors for PGP-1. (a) The visual high throughput screening of herbs against PGP-1. (b) The chromatogram of *P. corylifolia* as well as the prepared fractions 1-11. (c) Visual assay of the inhibitory effects of fractions 1-11 against PGP-1. (d) Three inhibitors from *P. corylifolia* and their inhibitory effects against PGP-1.

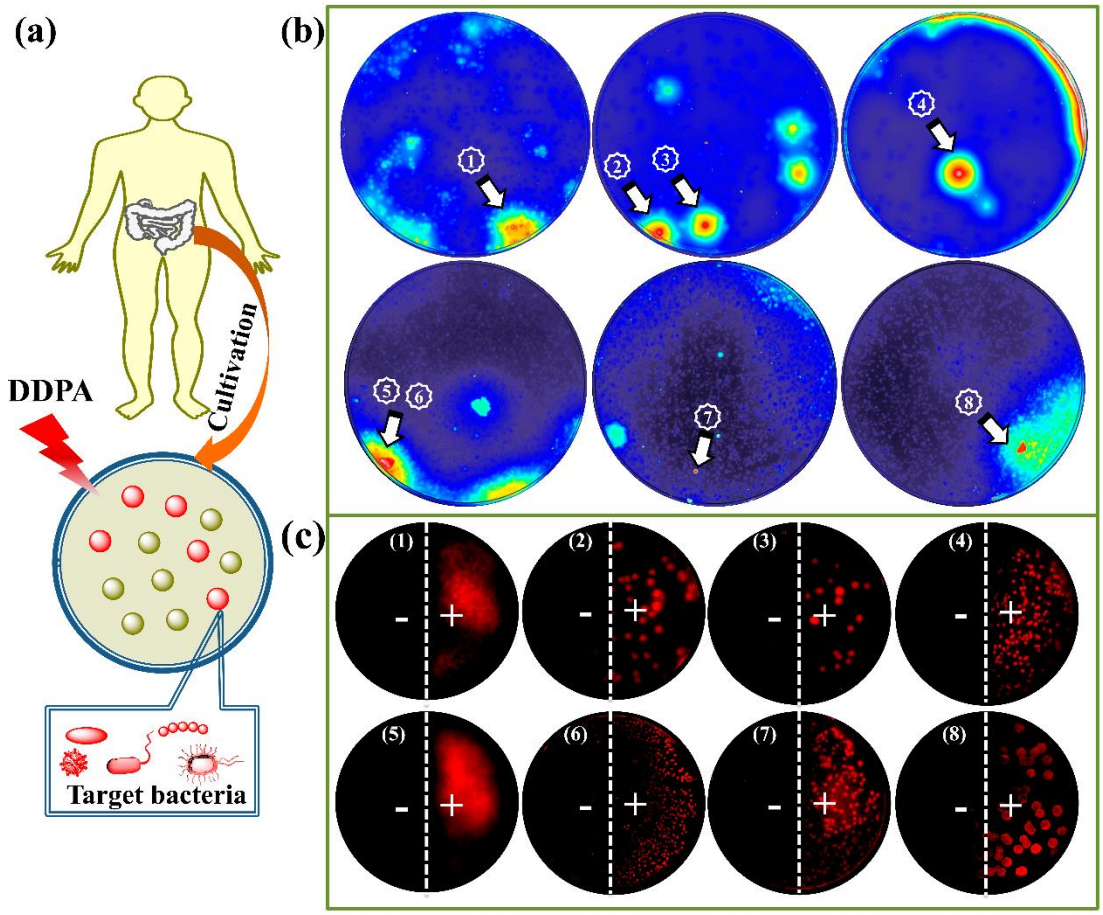

Fig. 4. Visual identification of intestinal bacteria from human feces using **DDPA**. (a) Illustration outlining the identification of target bacteria with active PGP-1 from human feces. (b) Fluorescence imaging of culture media for human intestinal bacteria cultivation using **DDPA**. (c) Visual sensing of endogenous PGP-1 corresponding to eight isolated intestinal bacteria using **DDPA**. (1) *K. pneumoniae* DSM 30104, (2) *K. pneumoniae* R-70, (3) *K. variicola* F2R9, (4) *K. aerogenes* NBRC 13534, (5) *S. flexneri* ATCC 29903, (6) *E. fergusonii* ATCC 35469, (7) *S. sonnei* CECT 4887, and (8) *B. velezensis* FZB42.

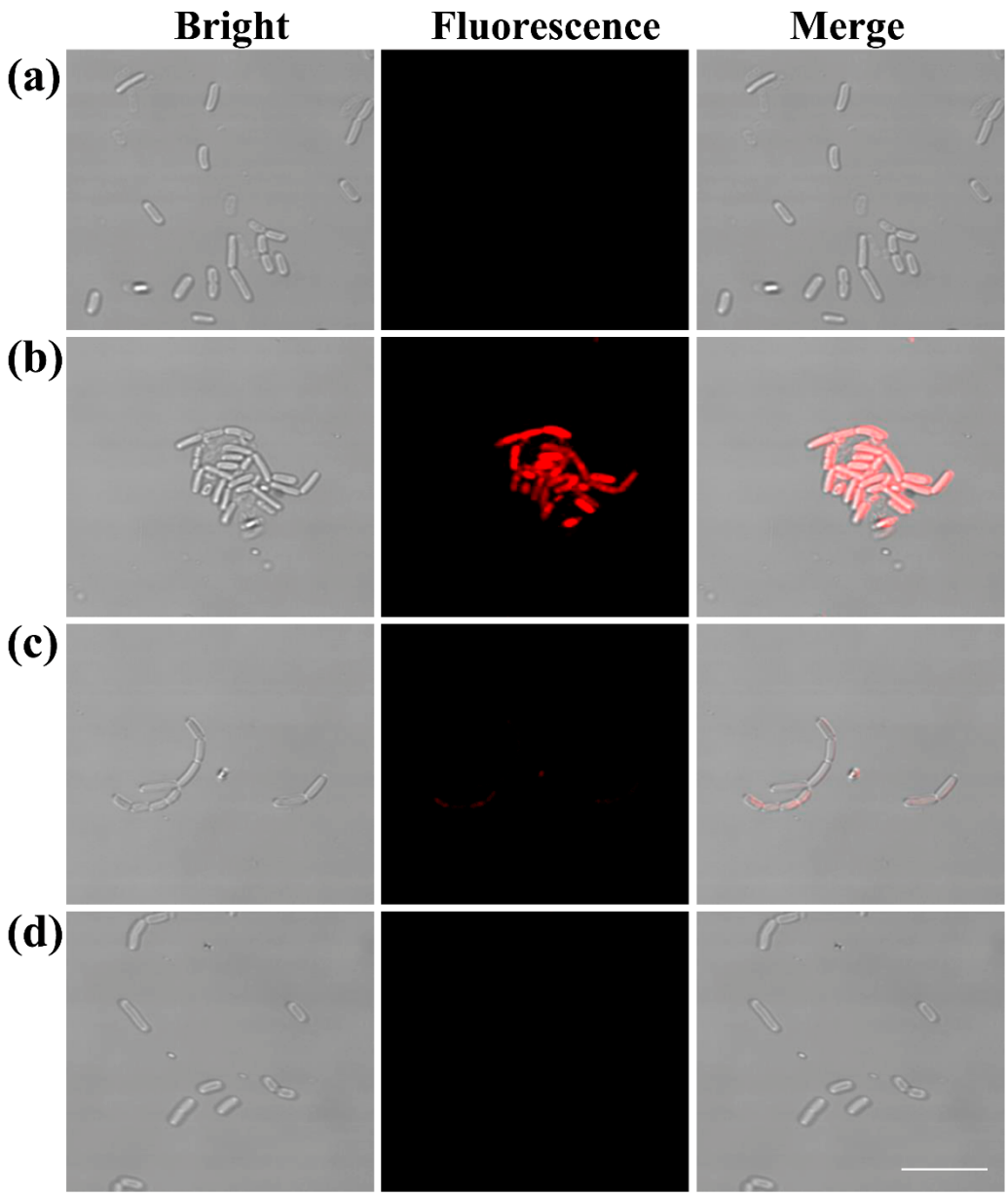

Fig. 5. Confocal laser scanning microscopic images of *B. velezensis* FZB42 (a) stained using **DDPA** (b), in presence of alantolactone (c) and bakuchiol (d). Scale bar 10 μm.